

Mechanical and Tribological Properties of CrN Coated Inconel X750

LIU Jiliang^{1,2}, LIAO Ridong^{1*}, LIAO Bin³, LUO Jun⁴, BAO Ke⁵

(1. School of Mechanical Engineering, Beijing Institute of Technology, Beijing 100081, China; 2. Beijing Liang Xin Technology Co., Ltd., Beijing 100081, China; 3. College of Nuclear Science and Technology, Beijing Normal University, Beijing 100875, China; 3. Beijing Radiation Center, Beijing 100875, China; 4. China North Vehicle Research Institute, Beijing 100072, China)

Abstract: Three CrN coatings were deposited on the Inconel X750 through the metal vapor vacuum arc ion implantation and the magnetic filtered cathodic vacuum arc deposition system (MEVVA-FCVA) with the N₂ flow rates of 10, 50, and 100 sccm, respectively. The surface morphologies and cross-section morphologies of the CrN coatings were obtained through scanning electron microscopy (SEM) and an optical profilometer. The microstructures of the coatings were characterized through X-ray diffraction (XRD). The hardness and the elastic modulus of the coatings were tested by a nano-hardness tester. The adhesion strength and friction coefficients were investigated through scratch tests and ball-on-disk tests and the wear tracks were tested by the optical profilometer. The experimental results indicate that the CrN coating deposited on the Inconel X750 substrate displays a uniform thickness and a smooth surface. The mechanical properties behaves well as the N₂ flow rate varies. The CrN coating significantly reduces the friction coefficient fluctuation and improves the anti-adhesion and anti-wear properties of the Inconel X750.

Key words: inconel X750; N₂ flow rate; CrN coating; mechanical properties; tribological properties

1 Introduction

The Inconel X750 is a well-behaved nickel-based alloy steel material. The Inconel X750 foil is often used in certain extreme harsh working environments, such as high temperature and corrosive environment^[1]. This material is ideal for air foil bearings^[2-4], turbine blades^[5] and springs^[6]. However, the Inconel X750 foil suffers from the friction and wear, chemical corrosion and high temperature oxidation during the practical utilization which leads to the early failure of parts and fails to meet the relevant service life requirements. The CrN coatings have been widely utilized in industrial field, due to the corresponding excellent oxidation resistance^[7-9], corrosion resistance^[10-15], low friction coefficient and anti-wear properties^[16-23]. Therefore, the

deposition of the CrN coating on the Inconel X750 foil improves the adaptability of the working environment which is important for the working life extension of the components.

The mechanical and tribological properties of CrN coatings were investigated in some works^[24-26]. Table 1 shows the relevant studies focused on mechanical and tribological properties of CrN coatings. It is particularly noteworthy that by changing the relative N₂ and Ar flow rates, all crystalline phases could be observed^[27]. These crystalline phases included the Cr, Cr+N, Cr+CrN_x, Cr+CrN, and the Cr₂N phases. Similarly, Subramanian, *et al*^[31] proved that the different N₂ flow rates deposition process could produce a wide range of phases, such as Cr, Cr₂N, and CrN. The grain size increased as the N₂ flow rate increased^[32]. Apparently, the microstructural changes might have a direct effect on the hardness, adhesion, friction efficient and wear rate^[33]. For different substrates, these effects might be different. Therefore, the effects of different N₂ flow rates in the microstructure, the mechanical behavior and the tribological performance of the CrN coatings on the Inconel X750 is needed to be investigated.

In this paper, a CrN coating was deposited on the Inconel X-750 through the metal vapor vacuum arc ion implantation and the magnetic filtered cathodic vacuum arc deposition system (MEVVA-FCVA). The surface

© Wuhan University of Technology and Springer-Verlag GmbH Germany, Part of Springer Nature 2019

(Received: Aug. 12, 2018; Accepted: Oct. 27, 2018)

LIU Jiliang(刘吉良): Ph D Candidate; E-mail: Liujiliang@beijingliangxin.com

*Corresponding author: LIAO Ridong(廖日东): Prof.; E-mail: liaord@bit.edu.cn

Funded by the Special Plan of Scientific and Technological Innovation for Graduate Student in Beijing Institute of Technology (2015CX10015), and the National Natural Science Foundation of China (51405455)

Table 1 Mechanical and tribological properties of CrN coatings in previous literature

References	Method	Substrate	Counterpart (ball)	Hardness/ GPa	Load /N	Velocity /(m•s ⁻¹)	Friction coefficient	Wear rate/ (mm ³ •N ⁻¹ •m ⁻¹)
Forniés, <i>et al</i> ^[27]	DC planar magnetron sputtering	Singlecrystal Si wafers	Wc-Wo	18	3	0.03	-	2×10 ⁻⁶ (Bias=-100V, f _{N₂} =40%)
Polcar, <i>et al</i> ^[7]	Low arc deposition technology	Hardened steel	Si ₃ N ₄ /Al ₂ O ₃	17	5	0.04	0.8/0.5	3×10 ⁻⁶ /1×10 ⁻⁶
Warcholiński, <i>et al</i> ^[28]	Cathodic arc-evaporation	HS6-5-2 tool steel	Alumina	32	10	0.06	0.54	0.65×10 ⁻⁶
Zhou, <i>et al</i> ^[29]	Arc ion plating	2024 Al alloy	Si ₃ N ₄	25	10	0.15	0.68	48×10 ⁻⁶
Cai, <i>et al</i> ^[30]	Plasma enhanced magnetron sputtering	17-4PH steel	Wc-Co	19.9	2	0.2	0.81	1.89×10 ⁻⁶
Aissani, <i>et al</i> ^[21]	RF magnetron sputtering	XC100 steel	100Cr6 steel	19.53	5	0.5	0.55	-
Jin, <i>et al</i> ^[26]	Closed-field unbalanced magnetron sputtering ion plating	Ti6Al4V alloy	Wc-Co	12.14	5	1.25	0.52	1.5×10 ⁻⁶

Table 2 Deposition process parameters for CrN coating deposition

Deposition Steps	Vacuity/Pa	Arc current/A	Negative bias/V	Substrate heating Temperature/°C	Deposition time/min	N ₂ flow rate/sccm
Cr deposition	2.5×10 ⁻³	100	200	200	5	0
CrN deposition	2.5×10 ⁻³	100	200	200	30	10/50/100

morphologies, the cross-section morphologies, the microstructure and the mechanical properties at different N₂ flow rates were studied. In addition, the tribological properties of the CrN coating and the Inconel X-750 substrate against the SiC ball were compared.

2 Experimental

2.1 Specimen preparation

In order to observe the mechanical and tribological performance of the CrN coated Inconel X-750, the Inconel X-750 foil with 0.16 mm thickness was selected as the substrate. The preparation process was as follows.

Blanking. The diameter of the ASTM 1045 steel was selected at 70 mm according to the installation requirements of the universal material tester (UMT). The plate was processed on the numerical control machine and the corresponding surface roughness was approximately 0.4 μm, as well as the thickness of 6.7 mm. The Inconel X-750 foil was cut with a diamond cutter to the size of 80 mm×80 mm.

Cleaning. To guarantee the cleanliness of the foil and the plate, both were cleaned by a detergent at first, and subsequently both were ultrasonically cleaned for 1 hour followed by a thorough drying.

Assembling. Two foils were placed on both the upper and lower surfaces of the plate, which could be

utilized to conduct experiments and guarantee the stress uniformity on these two surfaces during welding.

Diffusion welding. The vacuum bonding technology was adopted to ensure the surface smoothness of the specimen for welding. The welding temperature and loading pressure, which were critical to control parameters of the welding process, were set at 980 °C and 1 MPa, respectively.

Grinding. Following welding, the specimen was grinded on a cast iron plate through corundum powder addition with different sizes to ensure that the surface roughness of the specimen could reach 0.1 μm approximately.

Polishing. The 1/0.5 W diamond polishing paste was utilized to polish the specimen, where the surface roughness of the specimen could reach (0.04±0.02) μm approximately.

The CrN coating preparation was conducted by the MEVVA-FCVA composite systems. The deposition process is presented in Table 2.

2.2 Coating characterization

The cross-section morphologies of the CrN coating was measured by the S-4800 field emission scanning electron microscope (FE-SEM). The phase identifications was conducted through the X' Pert PRO MPD X-ray diffractometer (XRD) with a Cu Kα line. A nano-hardness tester (NHT²) was utilized to evaluate the hardness and the elastic modulus of the CrN coat-

ing and the substrate. A load of 20 mN was applied. The loading and unloading rates were 40 mN/min and the pressure holding duration was 5 s. The adhesion of the coatings was assessed through scratch testing by a reciprocating module of the UMT. The parameters were: cone angle of 120° , die diameter of 0.2 mm, load range of 1.5 N to 15 N, loading duration of 35 s and reciprocating module mobility of approximately 0.34 m/s. The UMT rotating module was utilized in the ball-on-disk tests for the tribological properties investigation of the Inconel X-750 foil against the SiC and the CrN coating against the SiC. The SiC ball diameter was 3.94 mm. The parameters in the test were: friction roller radius of 10 mm, rotation speed of 500 r/min, load of 5 N and duration of 30 min. The surface morphologies, the scratch tracks and the wear tracks were characterized by the NanoMap-D profilometer.

3 Results and discussion

3.1 Morphologies and microstructure

The SEM images of the cross-sections of the CrN coatings with different N_2 flow rates are presented in

Fig.1. It can be observed that the CrN coating thickness is uniform. The CrN coating thicknesses at the N_2 flow rates of 10, 50, and 100 sccm are 1.83, 2.14, and 2.38 μm , respectively. The thickness of the CrN coating increases with the increased N_2 flow rate, indicating that a higher amount of N_2 is ionized and a higher amount of CrN is formed during the same deposition duration. It also demonstrates that increasing the N_2 flow rate will increase the deposition rate of the CrN coating. Fig.2 presents the surface morphologies of the Inconel X750 substrate and the CrN coating with different N_2 flow rates. The results demonstrate that the surface roughness of the substrate increases with the CrN coating deposition^[31]. As the N_2 flow rate increases, the surface roughness are $0.05\pm 0.02 \mu\text{m}$, $0.07\pm 0.03 \mu\text{m}$, and $0.15\pm 0.05 \mu\text{m}$, respectively. Also, the number and depth of micropores formed during the deposition increases. This might be due to the accumulation of ions during the CrN coating deposition, which leads to an increase in the deposition rate. It could be observed from Fig.1 and Fig.2 that the CrN coated Inconel X750 exhibits good deposition results.

Fig.3 presents the XRD patterns of the CrN coat-

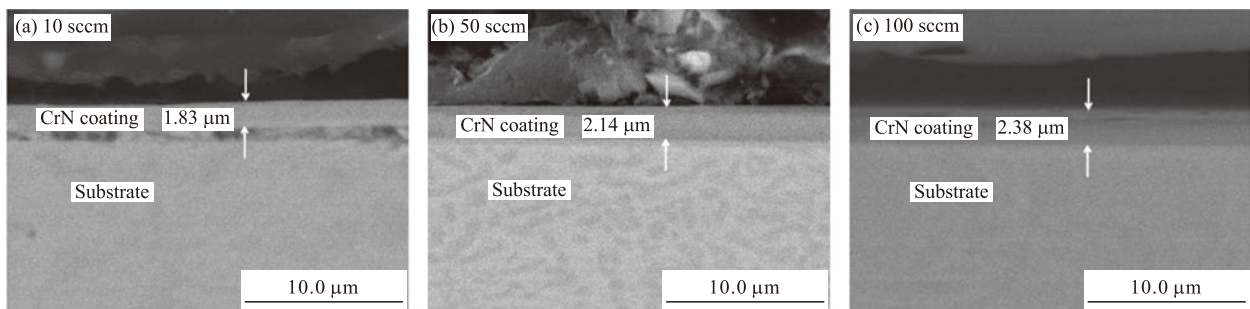


Fig.1 SEM images of cross-sections of CrN coatings with different N_2 flow rates

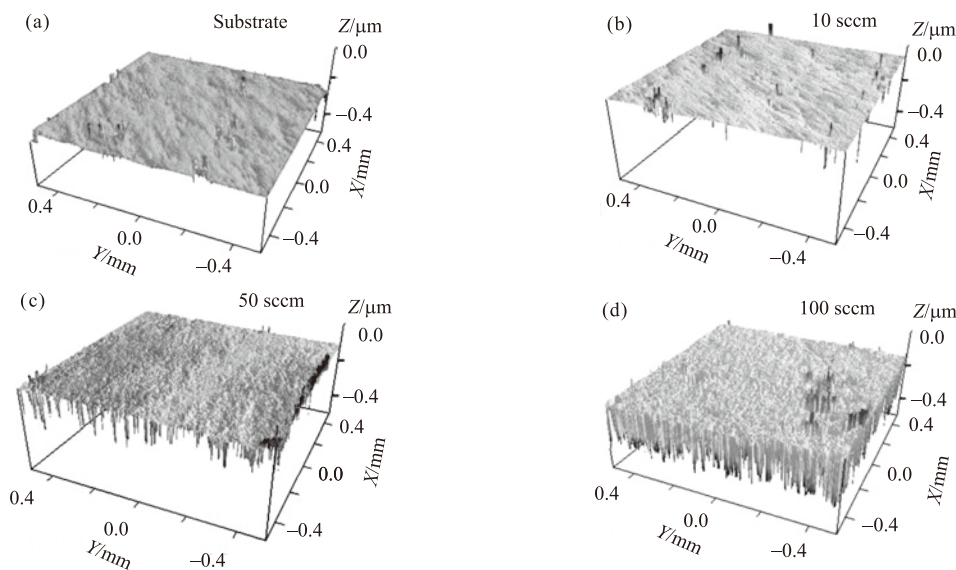


Fig.2 Surface morphologies of specimens

ings at various N_2 flow rates. The results demonstrate that the Cr (JCPDS 06-0694), CrN (JCPDS 11-0065), and Cr_2N (JCPDS 27-0127) phases can be formed through various N_2 contents during the deposition^[27,32]. The strong peaks appears nearly at 43.7° , 44.4° , 62.6° , 64.5° , 74.8° , and 81.7° and the corresponding crystal planes are CrN(200), Cr(110), Cr_2N (211), Cr (200), CrN(113), and the Cr(211). As the N_2 flow rate increases, Cr_2N (211) and Cr_2N (113) increases gradually, and Cr (200) is weakened. This indicates that as the N_2 flow rate increases, the nitrogen content increases. The Cr_2N phase is therefore enhanced and the Cr phase is weakened. This indicates that higher amounts of Cr and N is combined to form a Cr-N phase, leading to an increased amount of CrN formation simultaneously^[34]. This results are consistent with the observed results from SEM. The changes in these microstructures might have an effect on the mechanical properties of the CrN coatings.

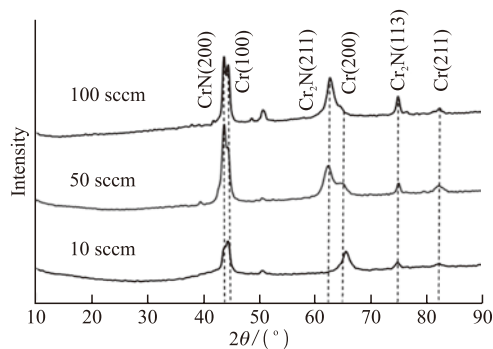


Fig.3 XRD pattern of CrN coating with different N_2 flow rates

3.2 Mechanical properties

Fig.4 presents the loading-unloading curves of one indentation on the CrN coating and the Inconel X750 substrate during the nanoindentation test. The Poisson ratios of the CrN coating and the substrate were 0.23 and 0.3^[35,36], respectively. The elastic modulus defined as the Ref.[37]:

$$\frac{1}{E_r} = \frac{1-\nu^2}{E} + \frac{1-\nu_i^2}{E_i} \quad (1)$$

where, E_r is the reduced elastic modulus of the contact, E and ν are the elastic modulus and poisson's ratio of the sample, E_i and ν_i are the elastic modulus and poisson's ratio of the indenter, respectively.

According to the Eq.(1) and relevant equations^[37,38], the average hardness and elastic modulus of the four indentations on the CrN coating and substrate were obtained. The relative results are presented in Table 3. As can be seen from Table 3, the average

hardness of the substrate and the CrN coating deposited substrates with the various N_2 flow rates of 10 sccm, 50 sccm, and 100 sccm are 8.31, 16.45, 23.79, and 23.72 GPa, respectively, indicating that the hardness of the deposited coating surface highly improves. The hardness of the CrN coating is almost the same when the N_2 flow rates are 50 sccm and 100 sccm which are significantly higher than that of N_2 flow rate 10 sccm. This is because the CrN (200) phase is formed for the preferred orientation, where the grain size is relatively high which can enhance the hardness. The average elastic modulus of the substrate and the CrN coating are 259.65, 261.75, 232.64, and 235.70 GPa with the N_2 flow rates of 10 sccm, 50 sccm and 100 sccm, respectively. The maximum reduced elastic modulus is 222.65 GPa with the N_2 flow rate of 50 sccm, which leads to the maximum elastic modulus.

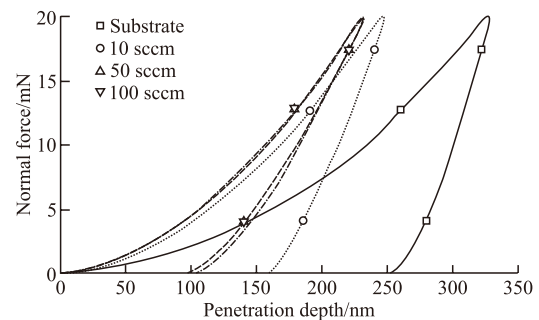


Fig.4 Load-unload curves

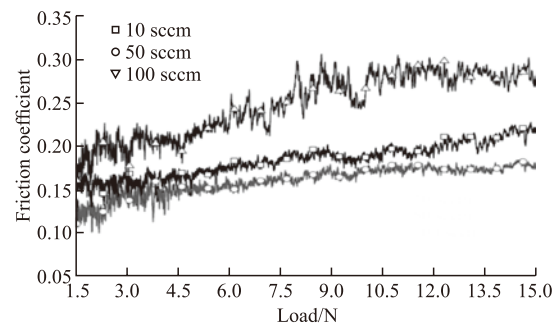


Fig.5 Friction coefficient measured during scratch testing

Table 3 Nanoindentation test parameters of substrate/CrN coatings with different N_2 flow rates

Parameters	Substrate	N_2 flow rate/sccm		
		10	50	100
Average hardness, H /GPa	8.31	16.45	23.79	23.72
Average elastic modulus, E /GPa	259.65	261.75	232.64	235.70
Average reduced elastic modulus, E_r /GPa	221.21	222.65	202.28	204.48
Unloading curve slope, S /($mN \cdot nm^{-1}$)	0.387	0.294	0.219	0.218
Maximum pressing depth, h_{max} /nm	328.31	248.36	232.39	232.68

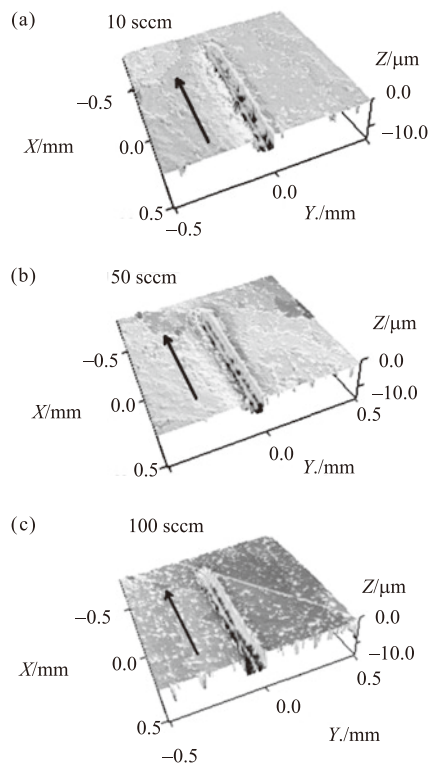


Fig.6 Scratch morphologies of from different N_2 flow rates of CrN coating near 15 N

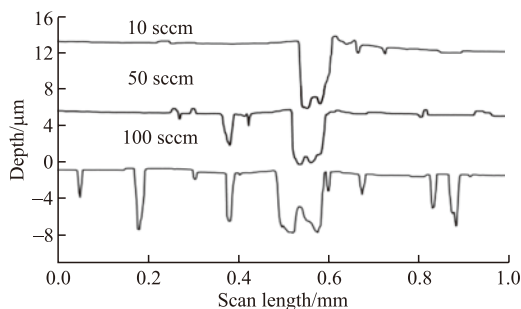


Fig.7 Section morphologies at $x=0$ in Fig.6

The adhesion strength of the CrN coating could be analyzed by scratch testing^[39,40]. The friction coefficients measured during scratch testing are presented in Fig.5. As presented in the figure, the friction coefficient at 50 sccm is relatively stable and a minimum value is apparent. This occurs mainly due to the higher hardness of the CrN coating. For the N_2 flow rate of 50 sccm, the tangential force during scratch testing is lower than that of N_2 flow rate of 10 sccm. However, for N_2 flow rate 100 sccm, due to the slight delamination of the CrN coating from substrate, the friction coefficient is bigger with the strong fluctuation. Fig.6 presents that the scratch morphologies of the CrN coating with different N_2 flow rates occurs at approximately 15 N. It is confirmed that the CrN coating is remained near the scratch tracks, as the corresponding friction coefficient appeared without any sudden change in Fig.5. This indicates the excellent adhesion of the CrN coating

onto the Inconel X 750 substrate with different N_2 flow rates. Fig.7 presents the section morphologies at $x=0$ in Fig.6. From the Fig.7, it can be apparently found that the deepest section morphology is about 5 μm with the N_2 flow rate of 10 sccm. This is because the CrN coating hardness is relatively low and the adhesive strength improves. As a result, the pressure head is easy to press the substrate. Also, when the N_2 flow rate is 100 sccm, the section morphology became quite wide. The width is up to 0.111 mm. This might be due to the increase in the number of micropores in the CrN coating, along with the increase in the width and depth of the micropores, resulting in a relatively severe removal of the coating during the scratch tests.

3.3 Tribological properties

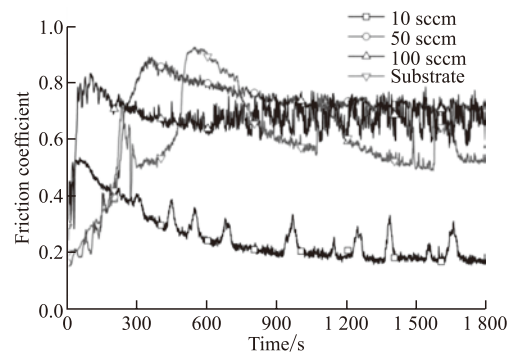


Fig.8 Friction coefficient in tribological tests

Fig.8 presents the friction coefficients of CrN coating against the SiC and the Inconel X750 against the SiC with different N_2 flow rates. From Fig.8 it can be observed that the friction coefficient variation generally experiences three stages, the rapidly increase, decrease and stabilization of the phases. In the first 600 s, the process can be considered in the run-in period. When the Inconel X750 substrate is tested against the SiC ball, the friction coefficient curve displays high fluctuation. This occurred due to the adhesive effect between the Inconel X 750 substrate and the SiC ball. When the N_2 flow rate is 10 sccm, it can be discovered that the stable friction coefficient reaches approximately 0.2, where the lower friction coefficient is observed. In contrast, a high number of peaks appeared on the friction coefficient curve. This might be related to the adhesion and material transfer of the secondary material during friction. Under the N_2 flow rate of 50 sccm it can be discovered that the friction coefficient is the most stable, and the stability value was approximately 0.7. When the N_2 flow rate is 100 sccm, the friction coefficient curve fluctuation is quite apparent. This is due to the reduction of the atomic percentage of Cr in

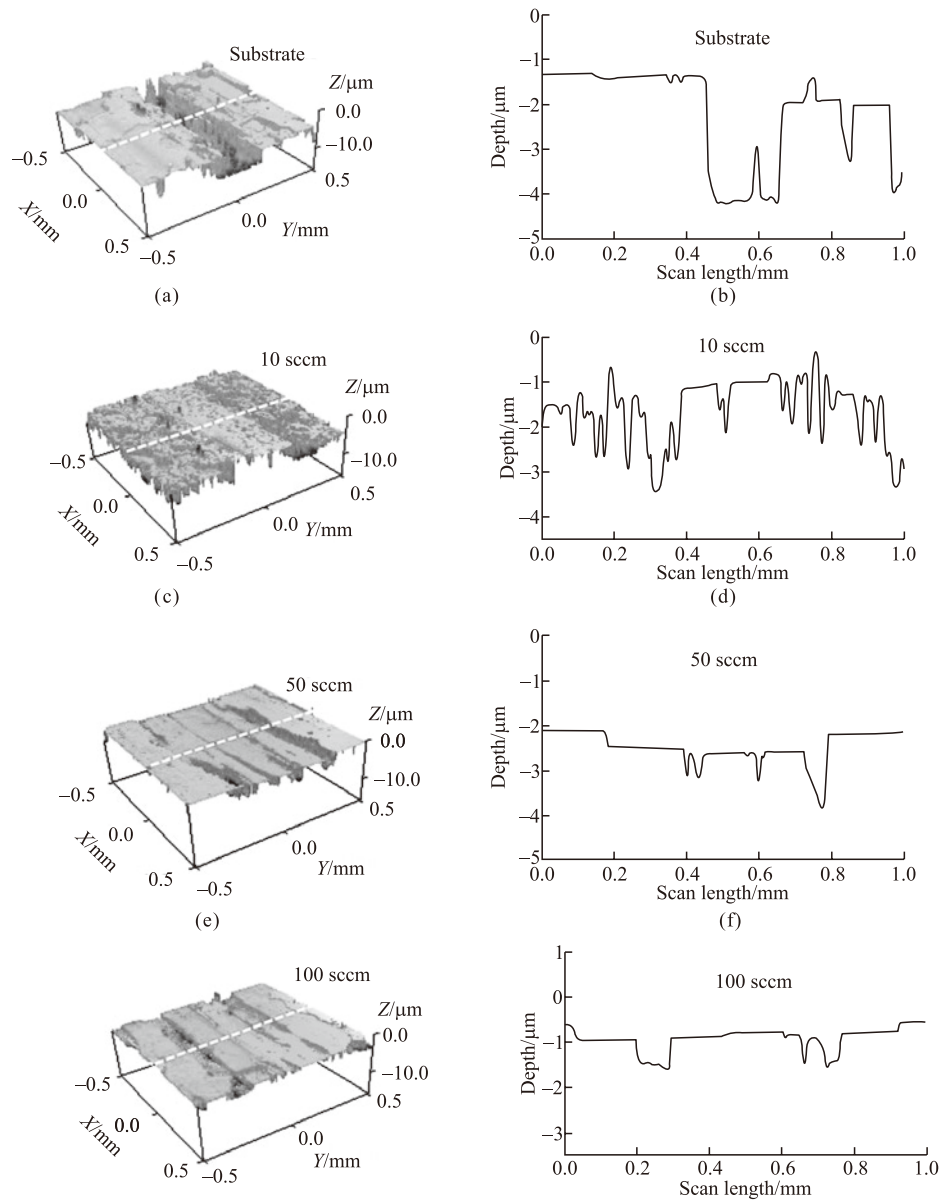


Fig.9 Micrographs of wear tracks and wear track profiles: (a) (b) substrate; (c) (d) 10 sccm; (e) (f) 50 sccm; (g) (h): 100 sccm

the CrN coating and the corresponding wear mechanism has changed. Under the low N_2 flow rate, the CrN coating is mainly composed of a metal phase, and the corresponding wear mechanism is mainly adhesive wear. The CrN coating is mainly a ceramic phase under a high N_2 flow rate, and the wear mechanism is mainly the abrasive wear. From the aforementioned results, the N_2 flow rate has significant effect on the friction coefficient.

In Fig.9, the micrographs of the wear tracks and wear tracks profiles following the tribological tests are presented. It can be observed that in the substrate the wear track shape is significantly apparent. The roughness on the wear track is also observed at the N_2 flow rate of 10 sccm, whereas the abrasion is significantly low at the N_2 flow rates of 50 sccm and 100 sccm. This

demonstrates that the anti-wear properties of the Inconel X750 are significantly enhanced when the CrN coating is deposited, especially at the N_2 flow rates of 50 sccm and 100 sccm, which is due to the higher hardness at that time frame.

4 Conclusions

a) The CrN coating has uniform thickness and smooth surface. As the N_2 flow rate increases, the surface roughness of the CrN coating increases. Also, the number and depth of micropores during deposition increases.

b) The N_2 flow rate has a significant effect on the CrN coating hardness and the maximum hardness is 23.79 GPa at the N_2 flow rate of 50 sccm. Through

scratch testing, the coating remains near the scratch tracks, but the width of the scratch tracks increases from 0.071 mm to 0.111 mm along with the increasing N_2 flow rate.

c) During the ball-on-disk experiments, the results indicate that the CrN coating effectively reduces the friction coefficient fluctuation, and improves the anti-adhesion and anti-wear properties of the Inconel X750 significantly. In order to obtain a stable and low friction coefficient, the optimum N_2 flow rate for the CrN coating should be between 10-50 sccm.

References

- [1] Altin O, Eser S. Pre-oxidation of Inconel Alloys for Inhibition of Carbon Deposition from Heated Jet Fuel[J]. *Oxidation of Metals*, 2006, 65(1/2): 75-99
- [2] Dellacorte C, Zalana AR, Radil KC. A Systems Approach to the Solid Lubrication of Foil Air Bearings for Oil-free Turbomachinery[J]. *Journal of Tribology*, 2004, 126: 200-207
- [3] Heshmat H, Hryniewicz P, Walton II JF, et al. Low-friction Wear-resistant Coatings for High-temperature Foil Bearings[J]. *Tribology International*, 2005, 38 (11/12): 1 059-1 075
- [4] Fanning CE, Blanchet TA. High-temperature Evaluation of Solid Lubricant Coatings in a Foil Thrust Bearing[J]. *Wear*, 2008, 265 (7/8): 1 076-1 086
- [5] Qureshi IN, Shahid M, Nusair KA. Hot Corrosion of Yttria-stabilized Zirconia Coating, in a Mixture of Sodium Sulfate and Vanadium Oxide at 950 °C[J]. *Journal of Thermal Spray Technology*, 2016, 25(3): 567-579
- [6] Judge CD, Gauquelin N, Walters L, et al. Intergranular Fracture in Irradiated Inconel X-750 Containing Very High Concentrations of Helium and Hydrogen[J]. *Journal of Nuclear Materials*, 2015, 457: 165-172
- [7] Polcar T, Parreira NMG, Novák R. Friction and Wear Behaviour of CrN Coating at Temperatures up to 500 °C[J]. *Surface and Coatings Technology*, 2007, 201(9/10/11): 5 228-5 235
- [8] Polcar T, Martinez R, Vitù T, et al. High Temperature Tribology of CrN and Multilayered Cr/CrN Coatings[J]. *Surface and Coatings Technology*, 2009, 203(20/21): 3 254-3 259
- [9] Wang L, Nie X. Effect of Annealing Temperature on Tribological Properties and Material Transfer Phenomena of CrN and CrAlN Coatings[J]. *Journal of Materials Engineering and Performance*, 2014, 23(2): 560-571
- [10] Shan L, Zhang Y, Wang Y, et al. Corrosion and Wear Behaviors of PVD CrN and CrSiN Coatings in Seawater[J]. *Transactions of Nonferrous Metals Society of China*, 2016, 26(1): 175-184
- [11] Ruden A, Restrepo PE, Paladines AU, et al. Corrosion Resistance of CrN Thin Films Produced by dc Magnetron Sputtering[J]. *Applied Surface Science*, 2013, 270: 150-156
- [12] Gilewicz A, Chmielewska P, Murzynski D, et al. Corrosion Resistance of CrN and CrCN/CrN Coatings Deposited Using Cathodic Arc Evaporation in Ringer's and Hank's Solutions[J]. *Surface and Coatings Technology*, 2016, 299: 7-14
- [13] Chen Q, Cao Y, Xie Z, et al. Tribocorrosion Behaviors of CrN Coating in 3.5wt% NaCl Solution[J]. *Thin Solid Films*, 2017, 622: 41-47
- [14] Basu A, Dutta Majumdar J, Manna I. Structure and Properties of CrxN Coating[J]. *Surface Engineering*, 2012, 28(3): 199-204
- [15] Shen LH, Cui QL. Synthesis of Cubic Chromium Nitride Nanocrystals Powders by Arc Discharge Plasma Method[J]. *Journal of Inorganic Materials*, 2010, 25(4): 411-414
- [16] Wang Q, Zhou F, WANG X, et al. Comparison of Tribological Properties of CrN, TiCN and TiAlN Coatings Sliding Against SiC Balls in Water[J]. *Applied Surface Science*, 2011, 257(17): 7813-7820
- [17] Su Y L, Yao S H, Leu Z L, et al. Comparison of Tribological Behavior of Three Films-TiN, TiCN and CrN-grown by Physical Vapor Deposition[J]. *Wear*, 1997, 213(1): 165-174
- [18] Podgornik B, Sedlaček M, Mandrino D. Performance of CrN Coatings under Boundary Lubrication[J]. *Tribology International*, 2016, 96: 247-257
- [19] Bandeira A L, Trentin R, Aguzzoli C, et al. Sliding Wear and Friction Behavior of CrN-coating in Ethanol and Oil-ethanol Mixture[J]. *Wear*, 2013, 301(1/2): 786-794
- [20] Zhou F, Chen K, Wang M, et al. Friction and Wear Properties of CrN Coatings Sliding Against Si_3N_4 Balls in Water and Air[J]. *Wear*, 2008, 265(7/8): 1 029-1 037
- [21] Aissani L, Nouveau C, Walock M J, et al. Influence of Vanadium on Structure, Mechanical and Tribological Properties of CrN Coatings[J]. *Surface Engineering*, 2015, 31(10): 779-788
- [22] Laxane R B, Bhide R S, Patil A S, et al. Characterisation of Chromium Nitride Physical Vapour Deposition Coating on Diesel Engine Pistons[J]. *Surface Engineering*, 2006, 22(1): 78-80
- [23] Etsion I, Halperin G, Becker E. The Effect of Various Surface Treatments on Piston Pin Scuffing Resistance[J]. *Wear*, 2006, 261(7/8): 785-791
- [24] Obrosova A, Sutygina A, Volinsky A, et al. Effect of Hydrogen Exposure on Mechanical and Tribological Behavior of CrxN Coatings Deposited at Different Pressures on IN718[J]. *Materials*, 2017, 10(563): 1-11
- [25] Wan S, Pu J, Li D, et al. Tribological Performance of CrN and CrN/GLC Coated Components for Automotive Engine Applications[J]. *Journal of Alloys and Compounds*, 2017, 695: 433-442
- [26] Jin J, Duan H, Li X. The Influence of Plasma Nitriding on Microstructure and Properties of CrN and CrNiN Coatings on Ti6Al4V by Magnetron Sputtering[J]. *Vacuum*, 2017, 136: 112-120
- [27] Forniés E, Escobar Galindo R, Sánchez O, et al. Growth of CrNx Films by DC Reactive Magnetron Sputtering at Constant N_2/Ar Gas Flow[J]. *Surface and Coatings Technology*, 2006, 200(20/21): 6047-6053
- [28] Warcholiński B, Gilewicz A, Kukliński Z, et al. Arc-evaporated CrN, CrN and CrCN Coatings[J]. *Vacuum*, 2008, 83(4): 715-718
- [29] Zhou F, Wang Y, Liu F, et al. Friction and Wear Properties of Duplex MAO/CrN Coatings Sliding Against Si_3N_4 Ceramic Balls in Air, Water and Oil[J]. *Wear*, 2009, 267(9/10): 1581-1588
- [30] Cai F, Huang X, Yang Q, et al. Microstructure and Tribological Properties of CrN and CrSiCN Coatings[J]. *Surface and Coatings Technology*, 2010, 205(1): 182-188
- [31] Subramanian B, Prabakaran K, Jayachandran M. Influence of Nitrogen flow Rates on Materials Properties of CrN(x) Films[J]. *Bulletin of Materials Science*, 2012, 35: 505-511
- [32] Cecchini R, Fabrizi A, Cabibbo M, et al. Mechanical, Microstructural and Oxidation Properties of Reactively Sputtered Thin CrN Coatings on Steel[J]. *Thin Solid Films*, 2011, 519(19): 6 515-6 521
- [33] Khojier K, Savaloni H, Zolghadr S, et al. Study of Electrical, Mechanical, and Tribological Properties of CrNx Thin Films as a Function of Sputtering Conditions[J]. *Journal of Materials Engineering and Performance*, 2014, 23(10): 3 444-3 448
- [34] Zhu SF, Wu YP, Liu TW, et al. Effect of N_2 Flow on Microstructure and Properties of CrNx Film Prepared by Unbalanced Magnetron Sputtering on the Surface of Depleted Uranium[J]. *Journal of Inorganic Materials*, 2012, 27(6): 603-608
- [35] Bouzakis KD, Vidakis N, Leyendecker T, et al. Determination of the Fatigue Behaviour of Thin Hard Coatings Using the Impact Test and a FEM Simulation[J]. *Surface and Coatings Technology*, 1996, 86: 549-556
- [36] Paouris LI, Bompos DA, Nikolakopoulos P G. Simulation of Static Performance of Air Foil Bearings Using Coupled Finite Element and Computational Fluid Dynamics Techniques[J]. *Journal of Engineering for Gas Turbines and Power*, 2014, 136: 022503-1-11
- [37] Broitman E. Indentation Hardness Measurements at Macro-, Micro-, and Nanoscale: A Critical Overview[J]. *Tribology Letters*, 2017, 65 (1): 1-18
- [38] Wang QZ, Zhou F, Yan JW. Evaluating Mechanical Properties and Crack Resistance of CrN, CrTiN, CrAlN and CrTiAlN Coatings by Nanoindentation and Scratch Tests[J]. *Surface and Coatings Technology*, 2016, 285: 203-213
- [39] Elangovan T, Kuppusami P, Thirumurugesan R, et al. Nanostructured CrN Thin Films Prepared by Reactive Pulsed DC Magnetron Sputtering[J]. *Materials Science and Engineering: B*, 2010, 167(1): 17-25
- [40] Wicinski P, Smolik J, Garbacz H, et al. Microstructure and Mechanical Properties of Nanostructure Multilayer CrN/Cr Coatings on Titanium Alloy[J]. *Thin Solid Films*, 2011, 519(12): 4 069-4 073